Parameters and some applications of plasma generated during keyhole welding using a highly concentrated energy beam – an overview

Georgi M.Mladenov[1], Dmitriy N. Trushnikov[2], Elena G.Koleva[3], Vladimir Ya. Belenkiy[4]

[1,3]Institute of Electronics, Bulgarian Academy of Sciences, Sofia1784, 72, Tzarigradsko shosee
[2,4]Perm National Research Polytechnic University, Perm, 614990, Russian Federation
[1,3]Technology center of Electron Beam and Plasma Technologies and Techniques, Sofia 1309, 69-70, ul. Vrania, ap.10

Abstract— *Keyhole welding using concentrated energy beams (electron beam and laser beam) is at the forefront of welding technology and finding ways to improve welding quality is a pressing issue. Finding optimal welding modes, monitoring weld quality and/or detecting weld defects in real-time during the welding process using nondestructive, cost-effective and reliable methods is one of current challenges. Plasma generated in the keyhole and the plasma plume (space above the welding pool) provides an opportunity to study welding stability and optimal modes as well as formation of weld defects.*

Generation and characteristics of plasma in the keyhole and above the welding pool are discussed in the paper. For laser keyhole welding spectral analysis data and video image techniques are widely used for control and inspection of laser induced plasma in real time. Electron beam welding is studied using plasma parameter measurements and by studying the current collected by the positively polarized ring electrode above the welding pool. In case of electron beam welding with beam oscillations the method of coherent accumulation is applicable to analyze of the plasma fluctuations process at the plasma electron current.

I. INTRODUCTION

Electron beam and laser beam welding are widely used technologies for joining of metals due to numerous advantages in comparison to other welding technologies. However, certain problems arise in the keyhole welding process, related to instability of weld joint formation and difficulties in creating and controlling the optimal welding modes. One of the main concerns of the industry is to assure the weld quality in real-time using a cost-effective and reliable method. It would be significant for the industry to be able to find optimal welding modes and/or detect defects non destructively in real-time during the welding process.

One of the phenomena that occur during interaction of concentrated energy beam with metal sample is generation of plasma in the welding zone. Study of plasma characteristics and their relation to process/product performance/quality could help increase knowledge of control of electron beam welding using concentrated energy beams and create approaches for its optimization. Due to the complex character of keyhole welding using high energy beams, differences in interactions of both beams with materials, and lack of adequate models of physical processes in the crater in the welding bath optimization and quality improvement of electron and laser beam welding technologies are empirical and still need more research.

II. PARAMETERS OF PLASMA, GENERATING IN THE INTERACTION ZONE OF INTENSE ENERGY BEAM WITH WELDED SAMPLE

2.1 Vacuum electron beam welding

During interaction between intense electron beam and metal low temperature plasma is generated in the welding zone [1-12].Deep penetration electron beam welding is associated with absorption of beam energy (over 5.10^5 W/cm^{-2}) by a work-piece through a capillary crater in the work-piece referred to as the keyhole. The keyhole is filled with metal vapor, ionized atoms and electrons. Vapor pressures in the keyhole near the root of the weld are higher thereby creating a vapor flow to the space surrounding the sample. Generation of plasma inside and outside the keyhole is a result of collisions of vapor atoms with beam electrons, electrons reflected by the sample wall and the generated x-rays. It can be assumed that in the root part of the keyhole due to concentration of ions (there are beam electrons and free electrons and ions, created by the ionizing processes) of order of 10^{17}– 10^{20} m^{-3} a compensation and/or overcompensation of the beam negative charge takes place temporarily or continuously(free electrons are loosed off the wall). In the next keyhole part due to

transportation of ions and mainly due to additional ionization of the ionized vapor flowing along the keyhole region, the electron concentration increases to 10^{22}-$10^{23}m^{-3}$[3] and Debye radius becomes less than the keyhole radius - i.e. ionized vapor achieves plasma state. Due to maximum plasma concentration in this deep part of the keyhole plasma parameters such as plasma potential and electron temperature are determined here. The Debye layer around the liquid metal walls of the keyhole keeps the balance between the numbers of plasma electrons and ions in the rest of the keyhole propagation distance. The flow of a mixture of hot neutral atoms and cold plasma ions, directed towards the orifice of the keyhole on the sample surface is controlled by gas-dynamic conditions in the keyhole and the concentration of these particles decreases. Then vapor cloud and plasma plume are emitted in the space over the welding zone [6-8]. Note that neutral atom distribution and plasma particle distribution over the welding sample surface are different due to different nature of their ensemble expansion.

2.2 Plasma parameters in case of vacuum electron beam welding

The plasma plume above the welding pool has been studied because it is readily observable.

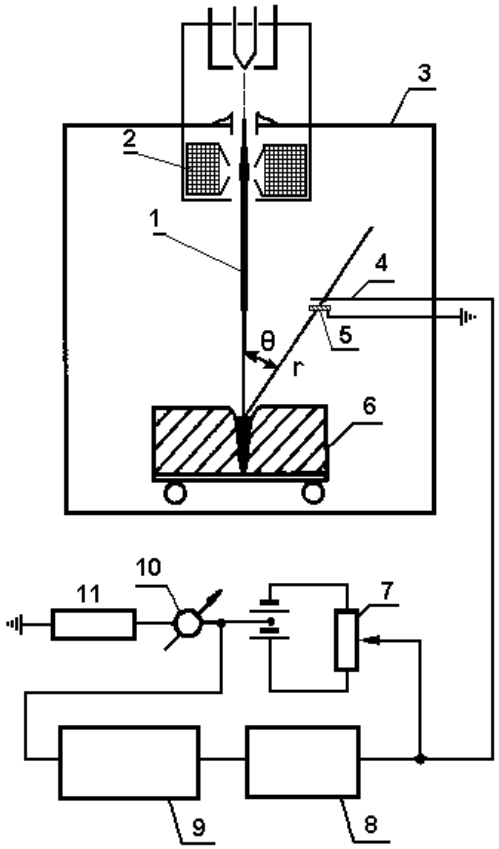

FIG.1. MEASUREMENTS OF PLASMA PARAMETERS DURING ELECTRON BEAM WELDING [4]

The plasma plume above the welding pool has been studied because it is readily observable. Some research used Langmuir probe methodology (the Langmuir probe is shielded from direct back scattered electron current by a grounded metal shield) [1,2,4,5,8],as shown in Fig.1. There 1 is electron beam, 2 - focusing coil, 3 – vacuum chamber, 4 - Langmuir probe , 5 – grounded metallic shield,6 - welded sample, 7 – two-polarity energy source, 8- logarithmic amplifier, 9 – recorder, 10 – measuring device, 11 – resistor.

At distances of 3-10 cm from the interaction zone electron temperature is kTe≈1-6 eV and electron density is of order of $10^{15}m^{-3}$(note, here density of neutral vapor atoms is of order of 10^{15} -$10^{16}m^{-3}$).In ref. [1,2] for Cu, Ni, Fe and Mo and semi-spherical welding pool (no keyhole penetration: U=13 kV; I=44 mA) density of charged particles at distances of 3-4 cm from welding bath is more than 10^{14}-$10^{15}m^{-3}$. The measured electron temperature there was 80 000 K-90 000 K. Plasma potential was 20-30V. Langmuir probe method was not applicable at higher beam powers due to oscillations of the probe characteristic data.

In ref. [4] at beam current of 10-70 mA and accelerating voltage of 25 kV, as in [4,5] at beam current of40-80 mA at accelerating voltage of 60 kV and welding velocity of 5-20 mm/s the density of charged particles is $10^{16}m^{-3}$, the electron temperature is 4 000 K at distances of 1-2 cm from the welding pool and the plasma potential is 3-4 V.Data accuracy is not high(with rate of mistake from 20% to 50%) due to oscillations of measured values, unclean surface of the probe in electron beam welding conditions and presence of negative ions or charged droplets. On Fig.2 to Fig.4electron partof volt-ampere probe characteristics is shown for three beam currents, three sample materials and two distances between welding pool and Langmuir probe. The ion part is not shown, because ion currents are more than 100 times smaller.

In ref. [5]electron temperature, density of charged particles and floating plasma potential are measured using the same Langmuir probe methodology at various beam parameters(beam current 40 mA, 50 mA and 60 mA; accelerating voltage 60 kV) and using various welding samples (Al, Ni, Cu). The results were as follows: electron temperature of plasma above the interaction zone Te was from 4 eV to 6 eV; density of charged particles in plasma plume Ne was from $10^{13}m^{-3}$ (for Cu), $10^{14}m^{-3}$(for Ni) and to $10^{15}m^{-3}$ (for Al); plasma potential Upl = 4 V.

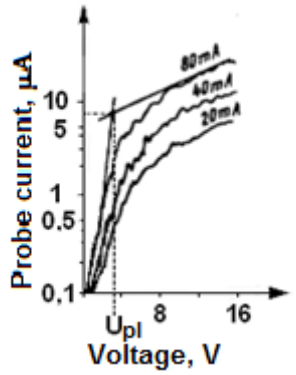

FIG.2. PROBE CHARACTERISTICS FOR THREE BEAM CURRENTS. THE DISTANCE TO WELDING POOL IS3 CM[4]

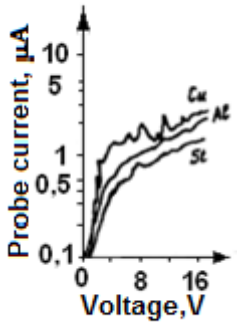

FIG.3. PROBE CHARACTERISTICS FOR THREE SAMPLE MATERIALS. IB=40 MA [4]

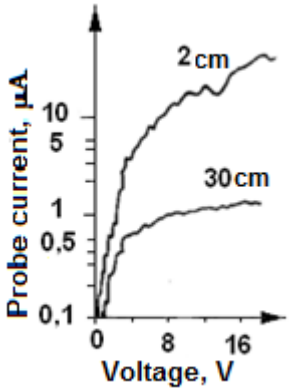

FIG.4. PROBE CHARACTERISTICS FOR TWO DISTANCES FROM WELDING POOL. IB=40 MA [4]

Discussing the two models – namely, hemispherical or cylindrical sources of free plasma expansion in the space over the beam-work piece interaction zone[6-8], it has been concluded [6] that a cylindrical plasma column in the region traced by the electron beam over the welding zone is formed. In ref. [8] oscillations of potential in the radial direction was predicted, due to different velocities of ions and electrons in the expanding plasma.

The relative distribution of the electron density and the electrostatic potential in the welding vacuum chamber were compared to experimental results and they showed good agreement.

2.3 Laser keyhole welding under atmospheric pressure

One of the best studied and most reliable methods to monitor laser keyhole welding is the analysis of detected plasma plume spectrum (Fig.5). This easy, non-contact, and inexpensive method can be automatized without difficulty in accordance with the required laser welding process. Spectral analysis is a useful method for acquiring desirable information during the laser welding process by recording the plasma spectral intensity with a spectroscopy sensor. The two main categories regarding the plasma diagnostic procedure are defined as direct and indirect methods. In the direct method (Thomson scattering and Stark broadening) [13], there is no assumption as to the type and degree of discharge equilibrium. The indirect method (Boltzmannplot and Sahajump) applies assumptions to the distribution of particles in the plasma region [14]. The Thomson scattering method has difficulties that are caused by its optical nature [15]. TheBoltzmann plot and Stark broadening are methods that have been typically used in a variety of studies [15]. The Boltzmannplot is a method that has been widely used in the electron temperature calculation flaser-induced plasma [16,17].

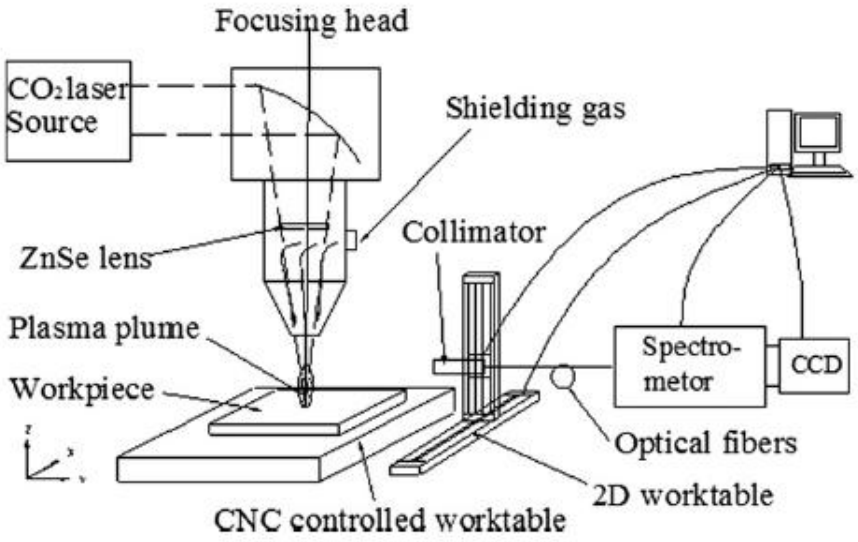

FIG.5. EXPERIMENTAL SETUP FOR PLASMA PLUME

In ref.[18]Szymanski and Kurzyna measured the emission spectra from plasma plume with a spectrograph during laser welding of stainless steel. The spatial variation of the plasma temperature was plotted on the assumption that the iron plasma was fairly symmetrical. They found that the whole temperature distribution of plasma plume appeared to be higher at the center and lower around it.

Laser-induced plasma in deep penetration laser welding is located inside or outside the keyhole – keyhole plasma and plasma plume respectively. The emergence of laser-induced plasma in laser welding reveals important information about the technological process of welding. Generally, electron temperature and electron density are two important characteristic parameters of plasma.

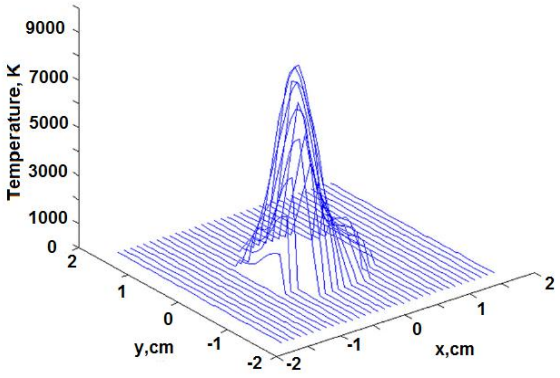

FIG. 6.ELECTRON TEMPERATURE FIELD OF THE PLASMA PLUME WITH AN UPWARD DISTANCE OF 2 MM FROM THE WORK PIECE SURFACE[19]

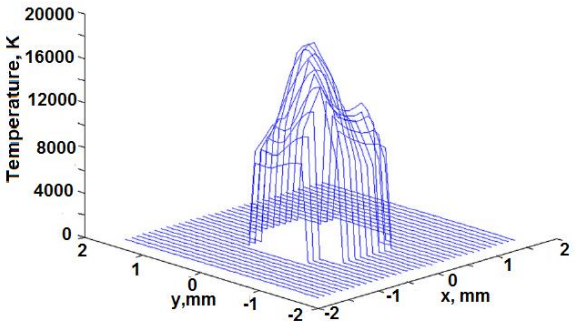

FIG.7. ELECTRON TEMPERATURE FIELD OF THE KEYHOLE PLASMA WITH A DOWNWARD DISTANCE OF 2 MM FROM THE WORK PIECE SURFACE[19]

In [19], spectroscopic measurements of electron temperature and electron density of keyhole plasma and plasma plume in deep penetration laser welding conditions were carried out on the assumption that the plasma was in local thermal equilibrium. Electron temperature of keyhole plasma is higher than that of the plasma plume (see Fig.6 and Fig.7). The maximum electron temperature in the key hole was 17,931 K generated at the centre of the keyhole plasma (Laser power was 1500W (CW) CO2 laser; the welding speed was 1.2 m/min; shielding gas was Argon at flowrate,0.5m^3/h).

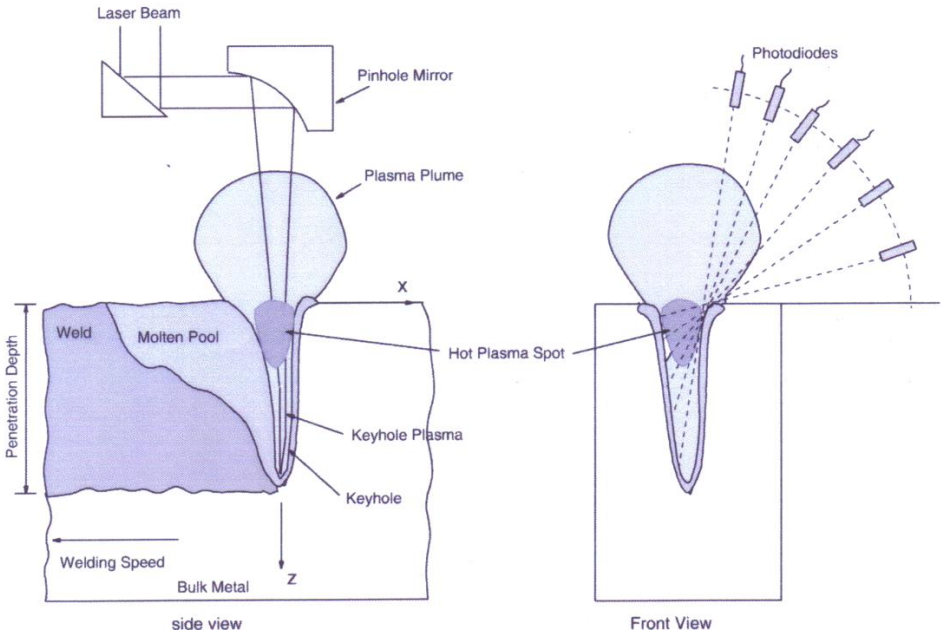

FIG. 8. SETUP FOR MONITORING KEYHOLE PLASMA DURING DEEP PENETRATION LASER KEYHOLE WELDING [8]

Miyamoto and Mori [20] proposed an idea to 'peak' into a keyhole using not one but several photodiodes arranged at different angles (Fig.8). Each photodiode provides a partial view into the keyhole and a photodiode can 'peak' deeper into the keyhole if it is arranged at a higher angle with respect to horizontal axis. By comparing the signals measured at different angles one can establish the plasma distribution inside in keyhole.

In [21] for 20 kW continuous wave CO2 laser, at welding speed of 2,7 m/min, assist. gas Helium, flow rate of 50 l/min, welded material – mild steel 25 mm thick, focus at 0 mm, and average keyhole depth of 9 mm the following were calculated. a) for plasma plume above the welding pool: from broadening the spectral lines Te=0,6795±0,0159 eV and from Boltzmann plot 0.689±0.207 eV; the electron density of the plume, based on the broadening of Fe 538.337nm as $0.632x10^{23}$ $m^{-3}$and based on Lorentzian profile $0.699x10^{23}$ m^{-3} respectively. The electron temperature inside the keyhole did not vary significantly, but a small increase (less than 10%) is observed at top portion of the keyhole. The electron density in upper 2-3 mm from the keyhole reaches $1,5x10^{23}m^{-3}$, while the electron density in the rest of the keyhole is about $0.3x10^{23}m^{-3}$. If this is compared to the electron densities of the plume and those inside the upper portion of the keyhole it will be found that plume electron density is two times less.

With the help of a spectrograph, plasma spectra in the keyhole are acquired [22] during deep penetration laser welding of aluminum alloy 6016 and the electron temperature and density (in the keyhole)are calculated. Results indicate that electron temperature is very unstable in the keyhole, which has a declining tendency in the radius direction (11 000 K to 8 300 K at keyhole walls) and Te on the keyhole depth fluctuates between about $0.4x10^4$ K and$1-1x10^4$ K as the keyhole depth changes from 1mm to 4mm. The electron temperature has a downward tendency as the laser welding keyhole depth increases. As is well known, the laser power at the lowest place of the keyhole is much higher than that at the uppermost place because of the keyhole effect. When plasma escapes from the keyhole, it is increasingly heated. So while the keyhole plasma electron temperature is10 000 K, it reaches 15 000 K just above the surface of the orifice. The electron density increases in the depth direction ($5.3-6.1x10^{21}m^{-3}$), while it does not change too much towards the radius ($5.2-5.3x10^{21}m^{-3}$). As the keyhole depth increases from 1mm to3 mm, electron density rises from $5.3x10^{21}$ m^{-3} to $6.2x10^{21}$ m^{-3}. The recoil pressure at the bottom is higher than that at the upper keyhole part, so ionization at the bottom is stronger than that at the top.

Concerning electron temperature during laser welding, different researchers may obtain different results. In some references [23,24,28–32,35], the electron temperature during deep penetration welding is less than10 000K,while in others [22,25,33], the electron temperature is more than10 000K.Finke et al. [23] carried out one-dimensional calculation with a cylindrical keyhole and pointed out that energy transferred from plasma to work piece due to the release of kinetic and recombination energies of electron-ion pairs is more effective than that by heat conduction at the surface of the material under their conditions.

Bhatti et al. [33] even got the highest electron temperature of over1x10^6 K. To explain the phenomen on Djebli [34] pointed out that plasma with two electron temperatures is common in many laboratory devices, where different temperatures of electrons are produced by two kinds of plasma sources. Besides, Bhattietal. [33] indicated that plasma parameters strongly depended upon the atomic number and surface binding energy of metals. Therefore it is not difficult to understand why the electron temperature is different in different articles. But referring to the relationship between plasma temperature and laser power, there is a contradiction: D'Angelo's [28] and Qi's [29] results showed that the maximum temperature of plasma increases with the growth of pulse laser energy, while Sibillano et al. [23] found that the electron temperature decreases as the laser power increases.

In ref.[36] during fiber LBW of aluminum alloy the electron temperature of 5300 K was measured. Electron density is in the range of 1.418 × 10^{24}m^{-3} to 1.636 × 10^{24}m^{-3} and ionization degree is no more than 1%. It was found that laser power of 5 kW is a turning point. After laser power reaches5 kW, the plume changes from metal vapor dominated weakly ionized plasma to strongly ionized plasma. The corresponding phenomena are the dramatic increase in the values of characteristic parameters and the appearance of a strong plasma shielding effect. Here, some Mg II ionic lines appear around the wavelength of 280 nm. The electron temperature (Fig.9a)., electron density(Fig .9b) and ionization degree of the plasma plume at laser power of 6 kW jump to 8448 K, 2.110 × 10^{24}m^{-3} and 25% respectively.

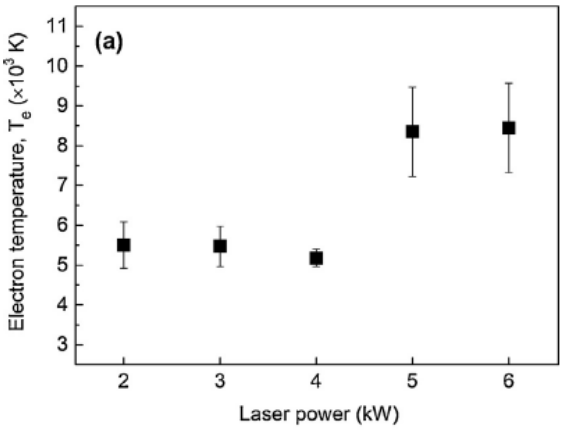

FIG. 9(A).ELECTRON TEMPERATURE OF PLASMA AS A FUNCTIONOF LASER POWER[36]

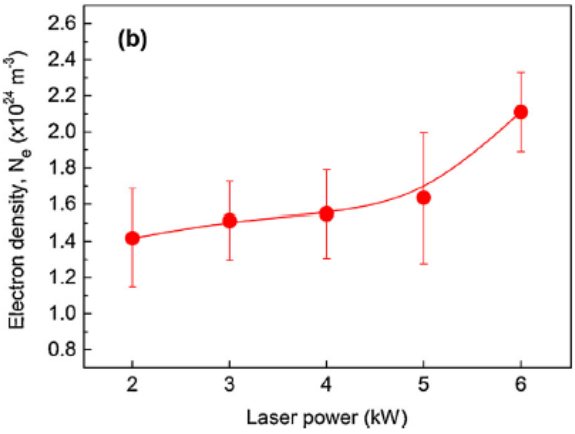

FIG. 9(B).ELECTRON DENSITY OF PLASMA AS A FUNCTIONOF LASER POWER[36]

As is seen in Fig.9 during LBW of aluminum alloy electron temperature was measured at 5300 K, electron density was in the range of 1.418 × 10^{24}m^{-3} to 1.636 × 10^{24}m^{-3}, and the ionization degree was no more than 1%. After laser power reached 5 kW, the plasma plume became characterized by strongly ionized plasma. Here, some Mg II ionic lines appear around the wavelength of 280 nm. The electron temperature, electron density and ionization degree of the plasma plume at laser power of6 kW jump to 8448 K, 2.110 × 10^{24}m^{-3}and 25%, respectively.

In ref.[37] for both continuous-wave laser and pulsed laser welding of zinc ''sandwich'' sample the average electron temperature of the zinc keyhole plasma was higher (10 000 K for pulsed laser and 6 000 K for continuous one) than that of the zinc plasma plume outside the keyhole (7 000 K for pulsed and5 000 K for continuous laser). In the welding process the continuous wave laser with higher input energy resulted in higher position of the zinc plasma with higher electron temperature above the sample surface (max 16 000 K for pulsed laser, 12 000 K for continuous-wave laser). More zinc vapor resulted in a higher average electron temperature of the plasma. In [38] experiment was conducted on fiber laser welding of galvanized DP980 steel by setting the laser power to 300W and welding speed to 1 mm/s. The calculated average electron temperature under these conditions was 7300 K. In the case of laser power of 2 500 W and welding velocity of 30-50 mm/s and the same steel, covered with zinc or not covered (v=30-50mm/sec) the Te was 9 000K and 7 500K respectively (from spectra of iron) and 28 000 K and 20 000 K (from spectra of zinc). The effect of weld speed on electron temperature is negligible. The sensitivity of electron temperature on the depth of weld penetration is ignorable.

In paper [39] based on the selected spectral lines, electron temperature and electron number density of plasma plume were calculated. (Te = 7 000 K – 13 000 K).

Optical emission spectroscopy [40] was also applied to analyze the plasma temperature and the electron number density in hybrid laser welding. The temperature and electron density distribution showed bimodal behavior (Te=10 000 K; Ne= $10^{23}m^{-3}$).

Plasma electron temperature was found [41] to decrease as far as laser power was increased together with the penetration depth in static as well as dynamic conditions. Such behavior does not correspond with an actual decrease of the plasma plume temperature but has to be attributed to the position of the optical collimator collecting light only from the top of the keyhole. Indeed, for deeper penetrations the hottest core of the plume moves down into the vaporized capillary so that the plasma temperature measured on top of the keyhole appears lower at higher incident powers. The electron temperature signal could be useful for development of a laser power feedback loop system to control the weld penetration depth. The calculated data are: Te=5 330 K – 5 650 K.

2.4 A comparison of plasma parameters during electron beam and laser beam welding

Note, that during vacuum electron beam deep penetration welding the generated plasma is weak low temperature plasma (measured using Langmuir probe) and during atmospheric pressure keyhole laser welding plasma is isothermal(light emission from exiting neutral atoms or ions is observed). The average plasma temperature in keyholes is found to be considerably higher than that in plumes in both types of energy sources. Plasma parameters in the keyhole are experimentally evaluated only for welds that are not very deeply penetrating.

Plasma plume outside the keyhole has been studied extensively in both types of concentrated energy beams because it is readily observable. Plasma above the welding bath in electron beam welding (EBW) is collisionless [6], because the mean free pathsle>10^3 cm and li>10^2cm even for maximal values of neutral and charged particle densities. In the beam region weak light emission from exiting vapor or residual gas atoms is sometimes observed. Plasma plume above the keyhole in case of laser welding is a bright, often bluish or green flash from isothermal light emitting plasma.

During deep penetration welding the plasma in the keyhole is in the temperature range of 4 000–80 000K.In ref.[36] as was mentioned above it was found that laser power of 5 kW is a turning point for plasma characteristics during laser welding. After laser power reaches 5 kW, the plume changes from metal vapor dominated weakly ionized plasma(ionization degree about 1%) to strongly ionized plasma(ionization degree reach 25%). Corresponding phenomena are the dramatic increase of the value of characteristic parameters and the appearance of a strong plasma shielding effect. Calculation of effective laser power density demonstrated that the plasma shielding effect is dominated in this case by inverse Bremsstrahlung absorption. The finding suggested that the plasma shielding effect must be considered in fiber laser welding of aluminum alloys, rather than ignored as claimed in several references concerning laser welding with laser power less than 5 kW.

No published data was found regarding plasma parameters in non-vacuum electron beam welding and in vacuum laser keyhole welding.

III. PLAZMA OSCILLATIONS AND SOME APPLICATIONS TO MONITOR LASER AND EB WELDING PROCESSES

3.1 Monitoring light emission from plasma in laser beam welding

In deep penetrating laser beam welding (LBW) study of keyhole instabilities is essential to understanding the welding process and appearance of weld seam defects [42-49]. In spite of extensive studying of spectroscopic characterizations of the plasma plume and of spatially integrated light intensity emission from the plasma plume only a few studies have so far focused on the description of its oscillations. Investigations of plasma plume image fluctuations are usually execute during one or more video cameras (Fig.10).

During the laser welding process the keyhole is kept open by the temporal pressure equilibrium. Keyhole shape and melt pool movement are undergoing forced instabilities and fluctuations at every violation of that equilibrium. These changes influence plasma plume dynamics and cause oscillations of plasma parameters. Assuming that fluctuations of the plasma plume are directly associated with melt pool and keyhole instabilities, examination of light signals emitted from the plasma plume is a tool for determining keyhole stability, transition of welding state and identifying defects.

In [42] high speed video observation and analysis of cause of periodic oscillations of plasma vapor flame with frequency of 2000-2500 Hz are discussed. These oscillations can be attributed to the oscillation of the keyhole. In paper [43] it is concluded, that the keyhole oscillates with frequencies higher than 500 Hz

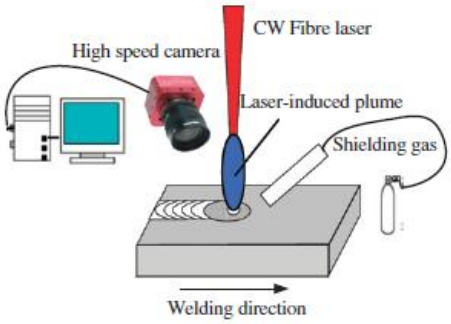

FIG.10. EXPERIMENTAL SET-UP FOR VIDEO OBSERVATION OF PLASMA PLUME

In ref. [46] the plasma/vapour induced during 4kW CW fiber laser welding of ZL114 aluminium alloy in the form of an 8mm thick plate is roughly divided into two parts: the keyhole plasma and the plasma plume. Keyhole plasma always exists, but its size and brightness change periodically. As its size increases, its brightness also increases. The plasma plume stays above the weldpool. Its size and brightness also change periodically, and it can be blown away by the gas flow. The plasma plume originates from keyhole plasma. Periodic change of the plasma plume is closely synchronized with that of keyhole plasma. Laser induced plasma/vapour oscillates periodically at cycles of 450–600 ms. Use of a shielding gas has little effect on the oscillation cycle. Plasma/vapour absorption is not the main reason for the periodic oscillation of plasma/vapour induced during fiber laser welding. Instead periodic oscillation of plasma/vapour can be largely attributed to oscillation of the keyhole opening.

In paper [48] LBW was performed on 12mm E-grade ship building steel plates using a 15kWCO2 laser, with helium as blowing gas. Plasma area, plasma radiation intensity and angle of plume were used as characteristics of plasma plume fluctuations and keyhole stability.

For analys is of the process of LBW in ref. [49] two high-speed cameras and a spectrometer were used. The authors managed to capture the plasma plume and the keyhole (where most of the process instabilities occur) during laser welding isochronously. Applying different image processing steps to the images taken by these two high-speed cameras the dynamic behavior of the process was detected. First the plume inclination angle β and the keyhole area were determined. Then frequency analysis was applied and discrete Fourier Transform computed with a Fast Fourier Transform (FFT) algorithm in MATLAB. There sulting single-sided amplitude spectrum was analyzed for every power step and as a result (Fig.11) characteristic frequencies were defined for every power step as the maximum frequency in the range of 0.5–3 kHz. At this dominating frequency there must be a change of the factors which determine keyhole characteristics and therefore plasma plume shape.

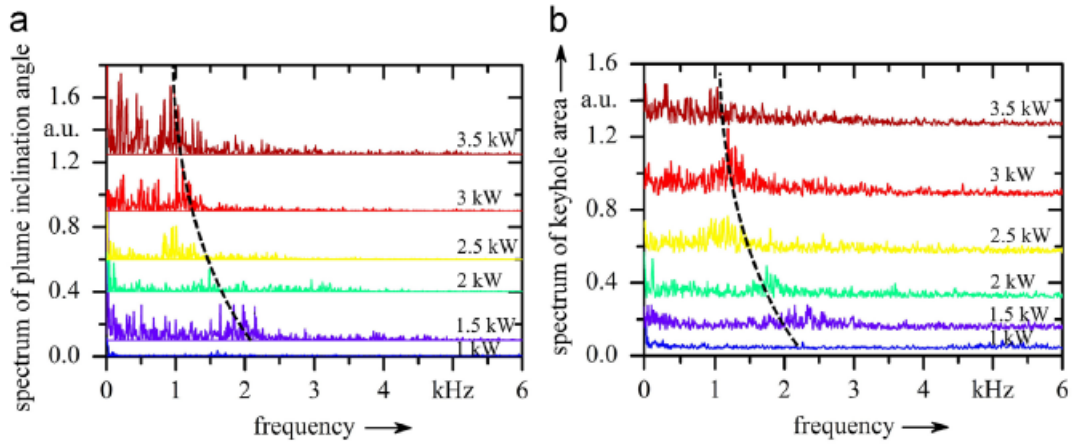

FIG.11.SPECTRA OF THE PLUME INCLINATION ANGLE (A) AND THE VISIBLE KEYHOLE AREA (B) FOR A CONSTANT FEED RATE OF 7 M/MIN ON ONE 5 MM STAINLESS STEEL PLATE. THE SPECTRA ARE PLOTTED TO SEPARATE THEM BEST, THE DASHED LINE INDICATES THE TREND OF THE DOMINATING FREQUENCIES (NO DOMINATING FREQUENCY VISIBLE FOR 1 KW).

Based on these figures a correlation between those two process characteristics (Fig.12) is derived. Additionally the plasma plume was imaged from two directions and volume of vaporized material the plasma plume carries was calculated (Fig.13). Due to these correlations the authors were able to conclude the keyhole stability. The authors were using the found correlation between the keyhole behavior and the plasma plume to explain the effect of the changing laser power and feed rate on keyhole geometry.

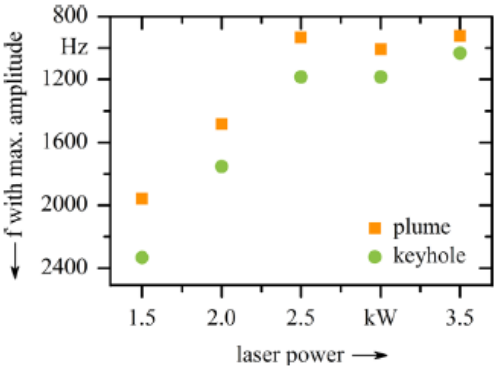

FIG.12. MAXIMA OF THE SPECTRA OF THE PLUME INCLINATION ANGLE AND THE KEYHOLE AREA IN DEPENDENCY OF THE LASER POWER (Y-AXIS IS REVERSED)

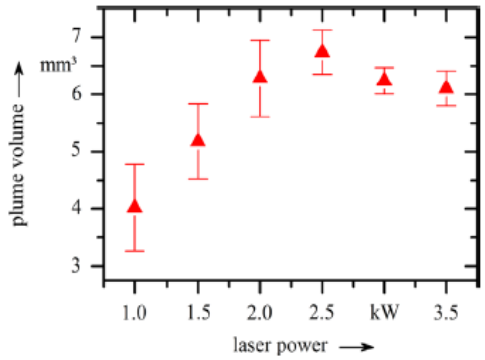

FIG.13. CALCULATED PLUME ESTIMATED VOLUME FOR DIFFERENT LASER POWERS AND A CONSTANT FEEDRATEOF7M/MINONTWO1MMSTAINLESSSTEELPLATES, N=3

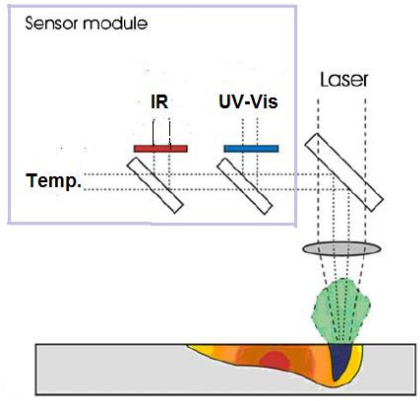

FIG.14 SETUP FOR COAXIAL OPTICAL RADIATION DETECTION [50]

The beam splitter mirror installed inside the laser head can help to transmit optical radiation signals from the welding area to the sensor [50]. Some of the welding statuses can be determined by analyzing the signal intensity of different spectral bands. Independent analysis of the features of different spectral bands is carried out by using different filter lenses. The light that travels through the filter is detected by the photodiode sensor, processed by the signal amplifier, and then data collected by the memory is obtained [51,52]. During the detection of the auxiliary light, it is preferred to use high frequency stroboscopic laser as light the source, and its waveband is set between 800 and 990 nm [53]. Video-camera and suitable filter, connected to one end of the beam splitter (in place of Sensor module in Fig.14) can provide an optical image of the laser induced plasma during the LBW.

3.2 Plasma charge electrical conductivity monitoring in laser keyhole welding

Electrical conductivity of the plasma plume had been utilized for monitoring laser induced plasma [54-56]. A contact probe, situated in plasma plume can be used to effectively measure plasma resistivity between the probe and the welding sample and thereby identify the welding status [55]. Second possibility is to use measuring circuits as follows: one end of the circuit is connected to the welding sample; while the other end is connected to the laser head (the welding sample and focus lens of the laser head should be electrically isolated). A load resistors (and capacitor) are used in the measuring circuit, and signals are

sent to the data processing system in the form of voltage [56]. In ref.[54] - see fig.15 - it is stated that by adding external voltage in series to the resistor ("+" on the nozzle and "–" is on the work piece) plasma current can be increased. Author had observed an increase of weld depth (namely increased efficiency of use of laser energy due to decreased energy absorption by the plasma). With increasing outer electric field intensity, there is a balance point at which the power efficiency is highest.

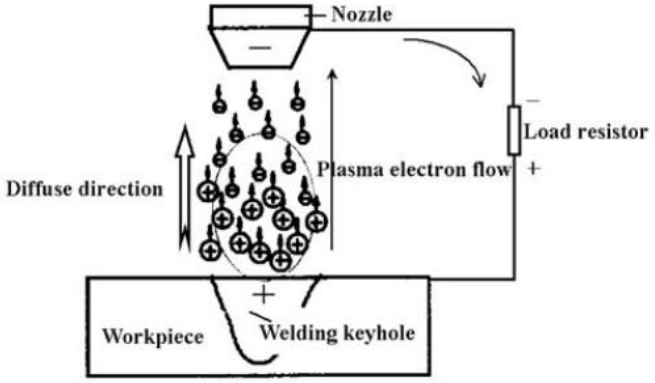

FIG.15. FORMATION OF THE PLASMA CURRENT CAUSED BY DIFFERENT DIFFUSION SPEEDS OF ELECTRONS AND IONS[54]

3.3 Secondary charged particles measurement in electron beam welding

From the beginning of application of the powerful electron beam for welding there were attempts to use the signals collected from charged particle flows above the welding zone to control the technological process. More clearly described was the research concerning detecting high-energy back-scattered electrons [57-60] or ions [60 - 62], collected above the melting pool. In many cases these studies were connected with measuring currents, collected at small positive potentials of a few volts. Many authors investigated the signal of collector [76], located above the welding pool and positively polarized. This collected current has for a long time been called secondary electron or thermionic emitted electron signal. On Fig.15 examples of signals [60] are given that were measured during EBW of steel at zero, small positive or negative potential (curves 1, 2 and 3). As usually these signals are distinguished by the authors of ref. [60] as back-scattered electrons, secondary electrons and ions. Note, that so-called secondary electrons signal 2exhibits behavior of collected back-scattered electrons1 (there is a sharp minimum at good beam focus and deep beam penetration. Explanation is that deep beam penetration in the welding sample leads to more difficult flow back of back-scattered electrons through the narrow keyhole). In the author's (of this review paper) opinion signal 2 is from the collected plasma electrons. At deep beam penetration distribution of plasma plume becomes more narrow (distribution around the beam being proportional to $\cos^3$ instead of cos from angle to vertical) and the ring collector electrode is situated in the periphery region of the plasma plume above the welding pool. Curve 3 (signal from collected ions) in case of sharp focusing has fluctuations at establishing keyhole. Vapor flow from the keyhole is wider and denser and the ions generating in the space above the welding pool in periphery of plasma plume are transported easily to the collector ring electrode (by collector electrical field and plasma boundary electrical potential drop). Here it is important that ion current signal is small and a small increase causes a big change.

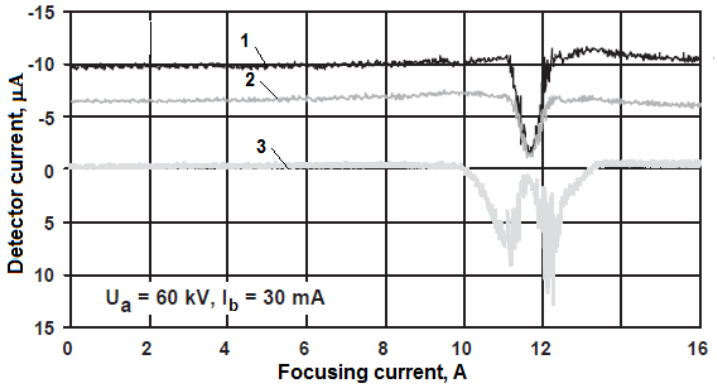

FIG.16. COMPONENT 0-50 HZ OF CHARGED PARTICLES' SIGNALS VS. FOCUSING CURRENT: 1-BACK-SCATTERED ELECTRONS; 2- SECONDARY (PLASMA PLUME) ELECTRONS; 3-IONS [60]

Fig.17 presents the spectra of signals, measured at conditions of Fig.16.

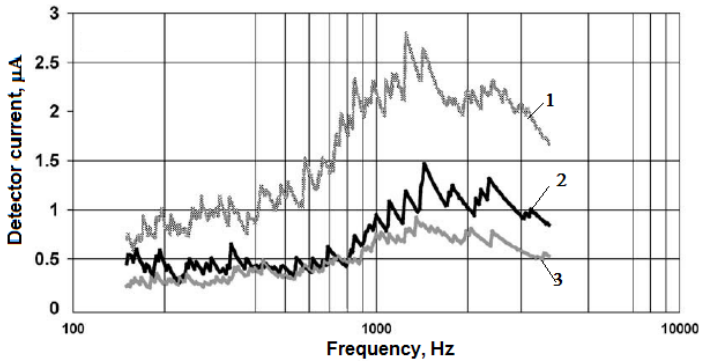

FIG.17. FREQUENCY SPECTRUM (COMPONENT 150 HZ-3 000 HZ OF COLLECTED CHARGED PARTICLES CURRENT AT EBW FOR CARBON STEEL (U_a=60 kV, I_b=30 mA) :1-BACK-SCATTERED ELECTRONS; 2-PLASMA PLUME ELECTRONS; 3-IONS[60]

In ref. [63,64] numerical simulations of plasma generation and transport during electron-beam welding process are presented and discussed. There is clear description of plasma formation in the case of polarization with positive potential (about +50 V) of a collector, set above the keyhole in the welding pool as well as the cases of zero or negative polarization of this collector. Positive collector potential due to plasma conductivity becomes plasma potential and plasma electrons are going to that electrode. At the same time thermionic emission occurs from keyhole walls pre-heated by the beam and that is keeping the balance between plasma electrons and plasma ions. In this case one could accept a non-independent discharge in the collector circuit [65-68]. In the cases of zero or negative collector potential the collector current is just the result of thermal diffusion of plasma particles in zone around the collector.

The spectrum of secondary current, collected by plasma could be divided into frequency ranges of 0-50 Hz; 50-3000 Hz and from 3-10 kHz to100 and more kHz. The first ranges are connected with keyhole wall axial and radial instabilities. The latter high frequency range is caused by generation of ion-acoustic instabilities in the plasma plume [69] between the keyhole orifice and the collector and is a subject of another discussion. Important conclusion from this study is that in order to avoid occurrence of ion-acoustic oscillations in plasma plume the collector must be situated at a small distance to the welding pool.

3.4 Experimental investigations of fluctuations of the collector signal of plasma plume electrons, generated during EBW

During electron beam deep penetration the keyhole shape is continuously influenced by the beam/work-piece metal interactions, leading to oscillations of the keyhole walls and instabilities of the melt pool. Experimental investigations show [70, 71] that the beam-keyhole system is a multi-parametric oscillating system with various feedbacks. This leads to local changes of heating and vaporization intensities, of angle of front keyhole wall, of channel shape and depth, and creation of such weld defects as pores and spiking.

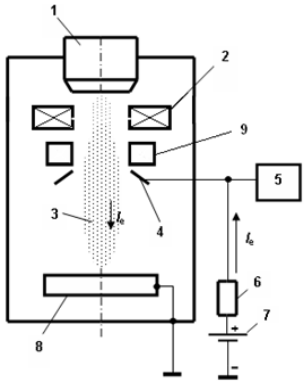

FIG.18. DIAGRAM OF SECONDARY ELECTRON CURRENT REGISTRATION IN PLASMA FORMED ABOVE THE AREA OF ELECTRON BEAM WELDING: 1 - ELECTRON GUN, 2 - FOCUSING LENS, 3 - PLASMA FORMED OVER THE AREA OF ELECTRON BEAM WELDING, 4 - ELECTRON COLLECTOR, 5 - A SYSTEM OF REGISTRATION, 6 - LOAD RESISTOR : 7 - A SOURCE OF BIAS, 8 – WORK-PIECE, 9-DEFLECTION COILS

The fluctuations influence the expanding plasma parameters [72].The fluctuations influence the expanding plasma dynamics and oscillations of the collecting plasma electrons. The frequency range below 5 kHz is associated with radial keyhole oscillations, and the range of up to 30 kHz with axial-azimuthal oscillations of the keyhole, mostly related to weld penetration.

Experiments in a series of papers were executed utilizing a standard electron beam welding machine (Fig.18). Accelerating voltage was 60 kV, beam current was 50 mA, and welding speed was 5 mm/s.

Graphic representation of the plasma current collected by a metal ring electrode with potential of+50 V, situated above the beam interaction zone (Fig.18) during electron-beam welding with a continuously operating beam can be seen on Fig.19.It looks as a series of high-frequency impulses which are modulated by low-frequency instabilities and follow each other in series almost regularly, reflecting focusing status of the beam.

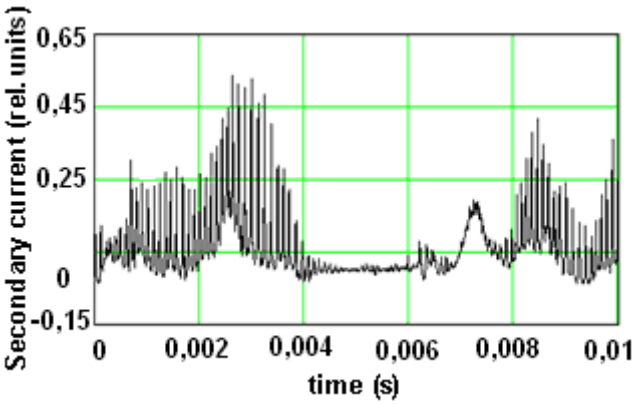

FIG. 19. TYPICAL RECORD OF THE COLLECTOR CURRENT, GENERATED BY PLASMA DURING EB WELDING. THE FOCUSING CURRENT PROVIDES SHARP FOCUSING OF BEAM; BEAM POWER IS 6 KW [67]

On fig.20spectrum of the plasma current (Fig.19) collected by the metal ring electrode4 (see fig. 18) is shown. This spectrum could be divided on the frequency ranges of: 0…5 kHz and 5 kHz…100 kHz.

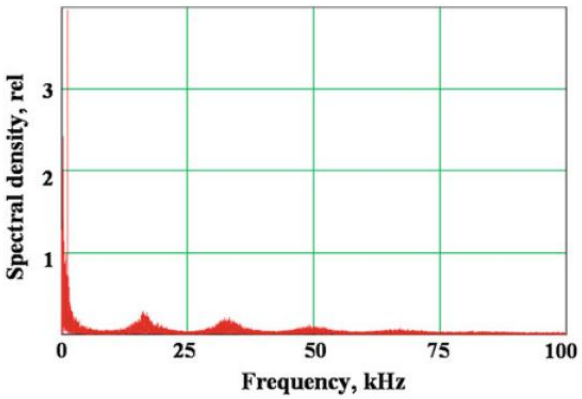

FIG. 20. SPECTRAL DENSITY OF THE SIGNAL OF COLLECTOR CURRENT AT FREQUENCIES F FROM 0 HZ UP TO 100 KHZ (STEEL WELDING WITH STATIC BEAM); POWER 3 KW; SHARP FOCUS MODE [67]

In [66-68] frequency range below 5 kHz is associated with mechanical radial and axially-azimuthal keyhole wall oscillations, and the range from 5 kHz up to about 15 kHz with processes such as vapor-plasma flows through keyhole and electrical and thermal non-linear interactions of the beam with these flows and keyhole walls. In [65] this signal range of oscillations is explained by local energy deposition and superheating of the metal surface, bombarded by the powerful beam and by consequent explosive destruction (ablation) of metal, as well as by instable electron emission from the bombarded surfaces on the keyhole walls. The spectral component with peaks of spectral density of the signal above 10 kHz as previously mentioned is caused by plasma ion-acoustic waves [69].

Such type of spectrograms is found almost at all welding modes with deep penetration of beam with power of 2 kW and more, for all the researched materials in several electron-beam systems (including systems without inverter power supply units).

3.5 Study of plasma plume density oscillations by measuring the signal, collected during EBW with beam deflection oscillations

An example of signal recording, collected from polarized to +50 V collector electrode by plasma plume (Fig.21) in the case of EBW with oscillations of the beam looks similar to recording on Fig.19 (curve 1). For comparison a recording of deflection coils current (curve 2) is also shown in the figure.

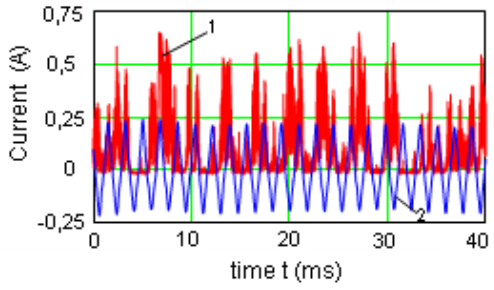

FIG.21. RECORDINGS OF THE CURRENT COLLECTED BY PLASMA AND OF THE CURRENT IN THE DEFLECTION COILS ARE SHOWN. WELDING OF STEEL WITH OSCILLATION ACROSS THE JOINT: P=2.5 KW, SHARP FOCUS (I_f=840 mA), OSCILLATION FREQUENCY F = 561 HZ, SWEEP SIZE 2A=0.9 MM. CURVE 1 PRESENTS HIGH FREQUENCY SERIES OF IMPULSES, PACKED IN LOW FREQUENCY OSCILLATION SIGNAL) AND CURVE 2 IS DEFLECTION COILS CURRENT [75]

Frequency spectrum of the current measured through the collector electrode polarized with +50 V shows that low-frequency oscillation component (0-3000 Hz) could be observed. It is assumed [73-75] that this mixture of random peaks(with amplitude reaching to 0.5 A) and low frequency signal fluctuations represents the free and the forced instabilities of the keyhole walls and plasma-vapor flows, and determines the plasma parameters near the collecting ring electrode.

For analyses of these signal oscillations in ref. [73-75] method of coherent accumulation is applied. The coherent accumulation method is illustrated on Fig. 22. The small-width square-wave signal formed from the signal from the deflection coils current (Osc(t)) is less than a basic signal g(t). The basic signal g(t + s) is shifted relative to the initial signal Osc(t) by a set time s.

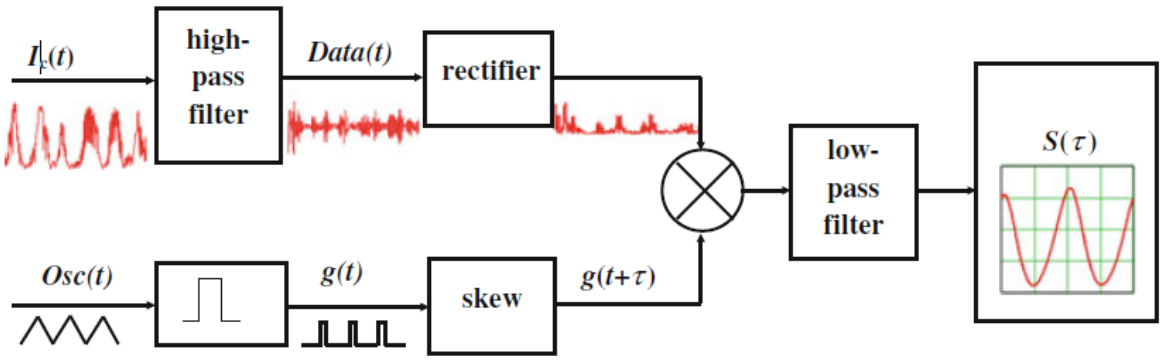

FIG 22. BLOCK-DIAGRAM OF COHERENT ACCUMULATION METHOD [73]

Authors find function S(τ) as follows:

$$S(\tau) = \int_0^{t_0} g(t+\tau) \cdot |Data(t)|\, dt$$

There t_o is sampling time. The function S(τ) expresses the average amplitude of the signal *Data(t)* for each value of the shift τ. The Method of coherent accumulation is based on Law of the large numbers and Central limit theorem of Probability theory.

As a result random fluctuations of the collector current are converted into well-defined probability of excitation of instabilities of the keyhole geometry.

Here are two examples of the S(τ) created by Coherent accumulation method during EBW of steel with oscillation across the joint (Fig.23 and along the joint- Fig.24 (P=3 kW, beam current 50 mA, oscillation frequency f= 630 Hz, oscillations sweep size 2A=1.5 mm).

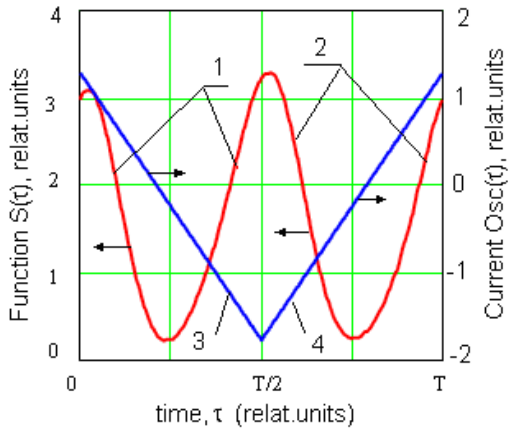

FIG.23. FUNCTION S(τ), OBTAINED BY COHERENT ACCUMULATION (CURVES 1 AND 2) AND OSC(τ) - RECORDING OF DEFLECTION COIL'S CURRENT (SEE STRAIGHT LINES 3 AND 4); THE PARTS 1,3 AND 2,4 OF THESE VARIATIONS ARE FOR ONE OF TWO DIRECTIONS OF THE BEAM MOVEMENT ACROSS THE KEY-HOLE. THE EBW MODE IS AS ON FIG.23[75]

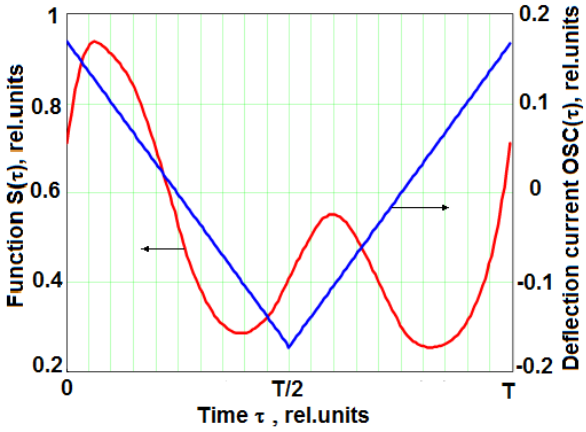

FIG.24RECORDING OF DEFLECTION COILS CURRENT SIGNAL OSC(τ) AND FUNCTION S(τ) OBTAINED USING THE COHERENT ACCUMULATION METHOD DURING STEEL WELDING WITH OSCILLATION ALONG THE JOINT (P=3 KW, BEAM CURRENT 50 MA, OSCILLATION FREQUENCY F= 630 HZ, OSCILLATIONS SWEEP SIZE 2A=1.5 MM)[75]

After treatment the obtained signal, collected by plasma in the process of welding with deflection oscillation across the joint, presented on Fig.23is practically symmetrical. There is also a small shift of positions of the maximal values of S(τ) in comparison to the positions of the changes of deflection coil's current directions.

The next S(τ) that is obtained using the method of coherent accumulation is shown on Fig.24. The result is for the study of welding with deflection oscillations along sample movement (and key-hole).The probability for excitation of oscillations of discharge parameters is bigger at times, when the beam is on the front keyhole wall. Conversely, this probability is characterized with a lower maximum (in comparison with the maximum at the front wall) at the times at which the beam is on the trailing keyhole wall. Minimum probability for excitation of oscillation of plasma signal is at times, when the beam is penetrating into the keyhole depth.

A rise of additional maximum in another place during keyhole crossing signifies detection of a weld defect. The time lag of maximal values of S(τ) is a function of focusing coil current and could be used for beam focus detection during the welding process.

3.6 Some results of numeric modeling of plasma in a vacuum chamber during EBW

In ref. [63,64,76] using a model for numerical simulation of plasma formation during vacuum EBW [63,64] useful data was obtained for various EBW conditions. Fig.25shows the relation of plasma concentration in the vacuum technology chamber to distance from the welding pool measured at 45 degree from the horizontal axis. There is no collector of electrons. Dots represent experimental data from ref. [6]. A good agreement can be observed. Fig. 26 shows electron density in the keyhole (negative values on the vertical axis). The ionization degree of plasma in the vicinity of the keyhole orifice is 10^{-2}, which is in good agreement with experimental data [6].

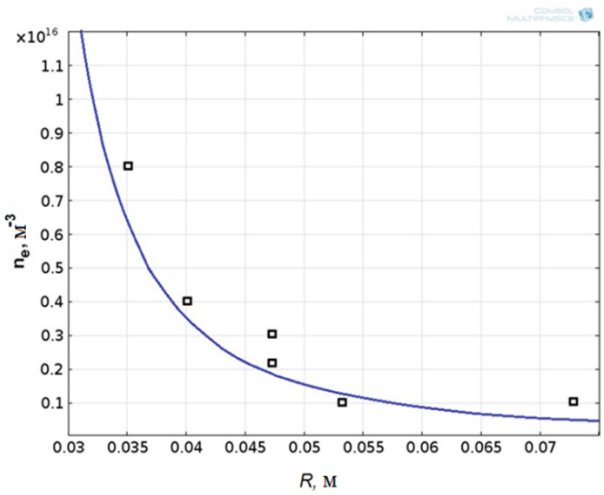

FIG.25. ELECTRON DENSITY IN THE VACUUM CHAMBER. THE DISTANCE R IS MEASURED AT 45 DEGREES FROM HORIZONTAL [63]

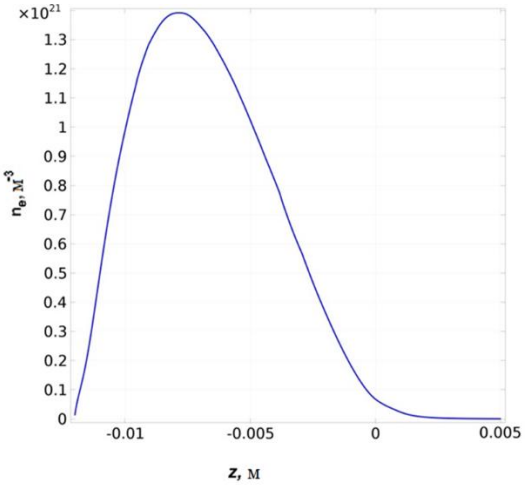

FIG.26. ELECTRON DENSITY OF PLASMA IN THE KEYHOLE. MAXIMAL VALUE IS $1.4x10^{21}$ m^{-3}. THE PENETRATION DEPTH IS 14 MM [63]

Electron temperature and plasma potential are at maximal values in the upper part of the keyhole (Fig. 27 and Fig.28). There calculated plasma potential is of order of 1.6-1,8 V and plasma temperature is about 4 000 K. This data is in good agreement with the experiments [4,6].

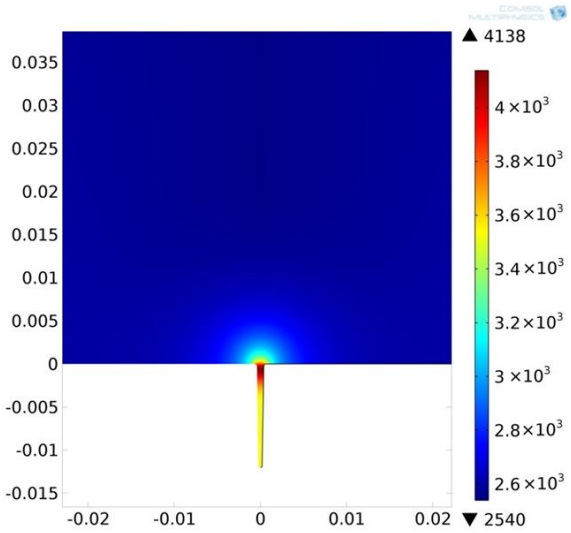

FIG.27.DISTRIBUTION OF ELECTRON TEMPERATURE (K) IN THE KEYHOLE AND IN VACUUM CHAMBER. THE DISTANCES ARE IN M [64]

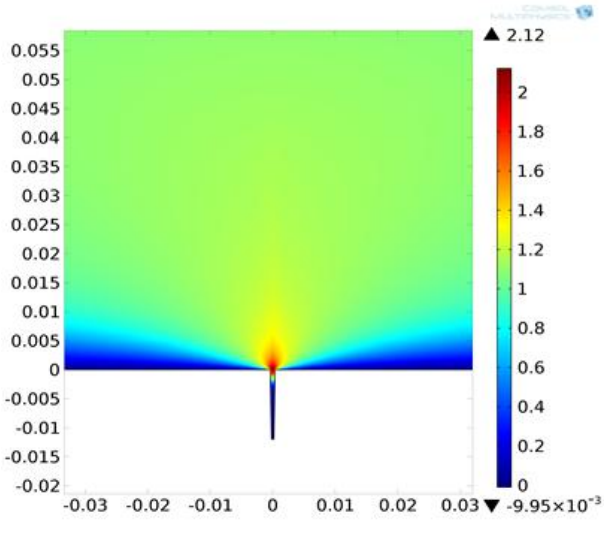

FIG.28. DISTRIBUTION OF POTENTIAL PLASMA (V) IN THE KEYHOLE AND ABOVE THE WELDING POOL. THE DISTANCES ARE IN M [64]

The model [63, 64] allows numerical experiments on plasma generation and behavior for the case of EBW with use of positively polarized (+50 V) ring collector of electrons [72-74]. In that case more visible are changes in the plasma potential distribution, determined by the collector potential value. Calculations were done for the loading resistor of 50 Ω. Fig.29 shows potential distribution in the keyhole and above the welding pool. The plasma potential in the space between the work piece and collector is about 25 V and collected plasma electron current is 0.5 A.

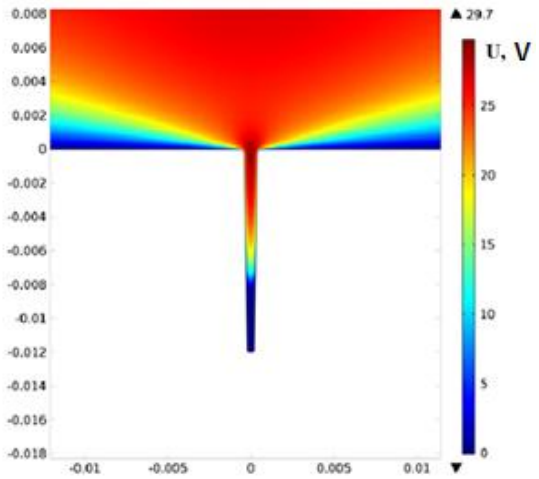

FIG.29. PLASMA POTENTIAL DISTRIBUTION IN THE CASE OF USE OF POSITIVELY POLARIZED COLLECTOR [64]

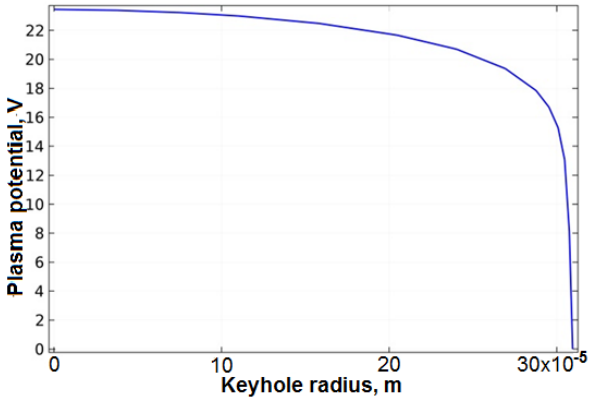

FIG.30 RADIAL DISTRIBUTION OF PLASMA POTENTIAL IN THE MIDDLE PART OF THE KEYHOLE [64]

Near the keyhole wall a very strong electric field is created (see Fig.30, Fig.31), due to existence of a very thin layer with a large potential drop (the electric field there reaches 10^6V/m). This strong electric field decreases the height of the potential barrier on the liquid metal surface. Electron emission in this case is described by the Richardson–Schottky equation:

$$j_t = AT^2 \exp(-e(\varphi - \sqrt{eE_k} / kT)$$

where E_k is the electrostatic field intensity.

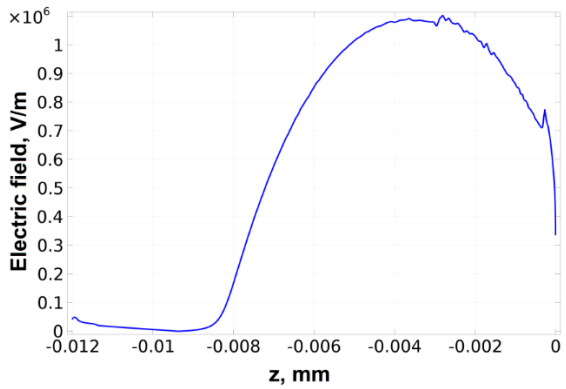

FIG.31. ELECTRIC FIELD DISTRIBUTION ON THE PENETRATION DEPTH Z NEAR KEYHOLE WALL [64]

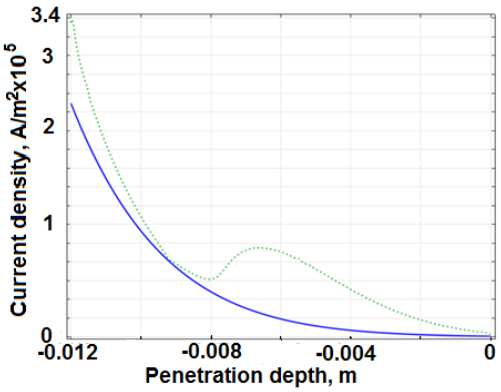

FIG.32. EMISSION CURRENT ON THE PENETRATION DEPTH:

—— j_{t0};…… j_t[76]

The thermionic current, calculated by Richards on–Schottky equation increases about tenfold around the keyhole orifice. This kind of emission currents density (j_t) sharply decreases when the electron beam interacts with bottom of the keyhole. Nevertheless due to strong dependence of emission current density (j_{t0}) on temperature the thermion emission from the bottom part of the keyhole is considerable, due to increase of temperature with increase of penetration depth-see Fig.32 [77,78]. A calculation of the emitted current, with the taking into account diffusion back movement of emitted electrons in the bottom part of the keyhole is shown on Fig.33. On the keyhole depth of about 9 mm and deeper the electron diffusion on the keyhole wall is dominated and direction of the current changes sign. Here electrical field is also reason for the emission drop.

On the Fig.34 plasma potential distribution in the keyhole and above the welded sample is simulated. Potential around the welded sample become near to 0 V and in the space around the collector it is about -50 V. The collected current is a function of ion density in space in front of the collector electrode and in the studied case is of order of 1 mkA.

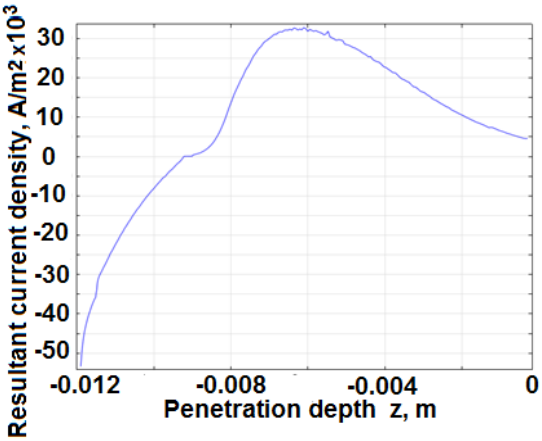

FIG.33 RESULTANT CURRENT DENSITY (ELECTRON EMISSION AND DIFFUSION) VS. DEPTH Z [76]

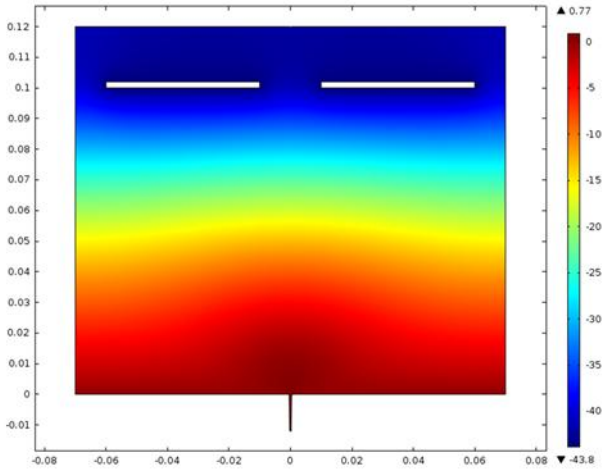

FIG.34. PLASMA POTENTIAL DISTRIBUTION (V) AT NEGATIVE POTENTIAL ON THE COLLECTOR [76]

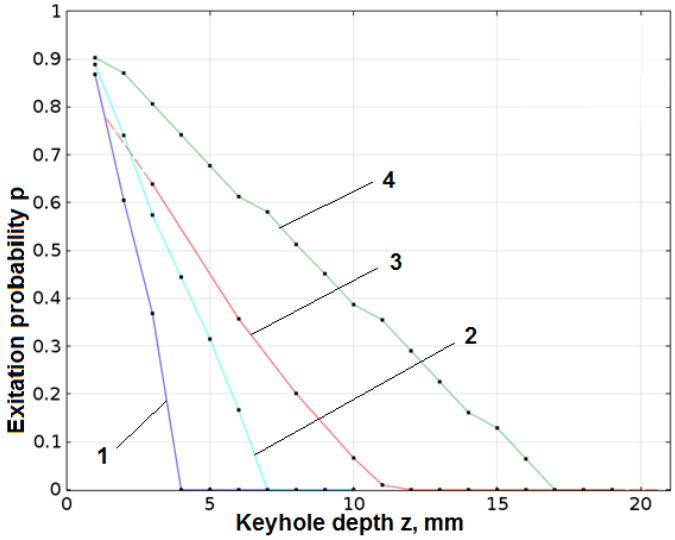

FIG.35. EXITATION PROBABILITY OF ELECTRONS, CREATED AT THE KEYHOLE DEPTH Z THROUGH KEYHOLE OF RADIUS: 1-R=0.18 MM, 2-R=0.203 MM, 3- R=0.345 MM, 4-R=0.428 MM [76]

In ref. [76] probability of electrons (thermion, true secondary, plasma) that are generated on some keyhole depth z, to propagate through the keyhole length z to keyhole orifice is calculated based on abovementioned model [63,64] and using COMSOL software package, assigning some value to the keyhole radius (Fig.35). From presented results one can see that electrons are decreasing in a linear law, reaching zero value on any keyhole length, which is a function of keyhole radius. With a narrow keyhole (r=0.18 mm) the keyhole depth, from which electrons can exit from the keyhole is 4 mm, while with a wider keyhole (r=0.428 mm) they can exit from a keyhole depth of 17 mm.

IV. CONCLUSION

In this paper recent studies are reviewed as well as some older ones that haven't been improved upon since their publication. The paper is focused on understanding the processes of plasma generation and transportation when welding using concentrated energy beams, as well as known attempts of use of these processes for monitoring the stability and quality of laser and electron beam welding.

In the case of vacuum electron beam welding the efforts are included in study of secondary particles behavior and of collected by plasma currents. Probably due to limitations of the vacuum chamber results of optical studies of emitted from plasma light are not published. Unfortunately investigations of plasma behavior for EBW at middle and atmospheric pressures were not found.

A model of plasma formation in the keyhole in the liquid metal and above the EBW zone has been described. Plasma parameters for keyhole and space above the welding pool were simulated. Thermionic electron emission was calculated for the keyhole wall. The calculated data is in good agreement with the experimental data. It is shown that there is a need to take into account the effect of the strong electric field in the keyhole near the keyhole wall on electron emission when calculating the current for non-independent discharge.

From reviewed papers one can conclude that optical sensing has become a mature real time monitoring technology for laser welding in laboratory and industrial practice. Photodiode sensors with advantages of low cost and simple structure provide rich information on high frequency features of the emitted light. This makes this method adaptable to larger scale industrial manufacturing. The visual camera gives a great deal of spatial information and has high accuracy in detecting weld defects. The spectrometer captures data for evaluating plasma characteristics during the laser welding process, which help to analyse welding stability and defects of the weld seam. Besides choosing a suitable filter system in video-imaging is considered the key step for obtaining accurate detecting information. Spectral analysis and optical images of plasma plume and of work piece surface in welding pool area are the work horses that are utilized to study stability and defects in laser keyhole welding process.

Signals obtained through different sensors can be preprocessed by way of signal and image processing technologies to extract signal features. It is based on this that classifier connecting feature characteristics and weld defects are setup to conduct quality inspection. Little research has been conducted on adaptive control during the welding process, and the controlled variables are mainly confined to more widely disperse low power laser system.

Nevertheless, it should be noted that real time detecting and controlling technologies for electron beam and laser welding are far from perfect, and the detecting accuracy for different welding statuses and defects is expected to be improved. Unfortunately, there is not a multitude of sensors available to detect all kinds of welding statuses and defects. Moreover, the hardware characteristics of the sensors, such as sampling frequency and resolution, need updating. The limited computing speed of intelligent signal processing and recognition technology also restricts wide use of real time detecting.

ACKNOWLEDGEMENTS

This work was supported by a grant from the Russian Foundation for Basic Research RFBR 14-08-96008 ural_a and with financial support for the base part of the state task of Russian Federation (No. 1201460538).

REFERENCES

[1] Ledovskoy V., Младенов G. About the parameters of the plasma generated by the electron beam in the process chamber, Izvestia LETI, v. 126, 1972, 96.(SanktPeterburgElectroingeneringInstitute, SanktPetersburg, Russia)

[2] Mladenov G. Ein Physikalisches - und Warmemodell des Elektronenschweissens, ZIS - Mitteilungen, Halle, DDR, N 1, 1978.

[3] RykalinN.N., I.V.Zuev, A.A.Uglov, book: Fundamentals of electron beam treatment of materials, Moscow, Mashinostroene, 1978, p239, (In Russian)

[4] Dyakov T., M. Bielawski, M. S. Kardjiev, B. E. Djakov, G. M. Mladenov, Electric probe studies of the ionizing metal vapor accompanying electron beam welding, International Conference on EB technologies, Varna, 1985, pp199-204.

[5] Kardjiev M., J. Besedin, G. Mladenov, Parameters of plasma produced from electron beam evaporation of metal targets, Proceedings of Fifth International Conferences on Electron Beam Technologies, EBT-97, Varna, Bulgaria, Publ. IE BAS, 1997, pp. 155-159.

[6] KrinbergI. A., G. M. Mladenov, Formation and expansion of the plasma column under electron beam-metal interaction, Vacuum, 77, 2005, pp.407-411.

[7] HoC. Y., M. Y. Wen, and C. Ma, Plasma from EB evaporation of a Metal Target, Advanced Materials Research, v.83-86, 2010, pp.1190-1196.

[8] Ho C. Y., M. Y. Wen , Y. H. Tsai , and C. Ma ,Potential and electron density calculated for free expanding plasma by an electron beam, J. Appl. Phys. 110, 013306 (2011). http://dx.doi.org/10.1063/1.3606581

[9] MladenovG. and S. Sabchevski, Potential distribution and space-charge neutralization in technological intense electron beams-an overview, Vacuum, 62 (2001), 113-122.

[10] TokarevV. O., O. E. Ostrovskii, V. A. Kazakov and I. V. Alekseev, Control of low- temperature plasma when electronbeamwelding non- ferrous metals and their alloys in an intermediate vacuum, Welding International, 9,12,1995, pp. 987-988.

[11] Novokreshchenov V.V., R.V.Rodyakina, Yu.V.Myakishev, A.P.Sliva, Determination of the degree of ionization of the vapor phase of the penetration channel in electron beam welding, Welding International, 2013v.27, No3, 238-242

[12] Ледовской В., Г.Младенов. Учет влияния плазменых явлений на взаимодействие мощных электронных пучков с веществом, Ж Т Ф, т 40, N 10, 1970, 2260.

[13] Torres J, Jonkers J, Van De Sande MJ, Van Der Mullen JJAM, Gamero A, Sola A. An easy way to determine simultaneously the electron density and temperature in high-pressure plasmas by using Stark broadening. J Phys D: Appl Phys 2003;36:L55–9.

[14] Griem HR. Principles of Plasma Spectroscopy. Cambridge, UK: Cambridge University Press; 1997.

[15] Liu L, Hao X. Study of the effect of low-power pulse laser on arc plasma and magnesium alloy target in hybrid welding by spectral diagnosis technique. J Phys D: Appl. Phys. 2008;41:1–10

[16] Sibillano T, Ancona A, Berardi V, Lugara PM. A real-time spectroscopic sensor for monitoring laser welding processes. Sensors 2009;9:3376–85.

[17] Greses J, Hilton PA, Barlow CY, Steen WM. Spectroscopic studies of plume/ plasma in different gas environments. Jacksonville, FL: Laser Institute of America, ICALEO; 2001.

[18] Szymanski Z,KurzynaJ. Spectroscopic measurement so laser induced plasma during weldingwithCO2 laser. Journal of Physics D:Applied Physics 1994;76(12)pp.7750–6

[19] ChenG. , M. Zhang , Z. Zhao, Y. Zhang, S. Li , Measurements of laser-induced plasma temperature field in deep penetration laser welding, Optics & Laser Technology 45 (2013) pp. 551–557

[20] Miyamoto I., Mori K. Development of in-process monitoring system for laser welding, Proc. ICALEO'95 , Orlando,Fl.Laser Institute of America, pp.759-67

[21] Tu J.F., Inoue T., Miyamoto I. Quantative characterization of keyhole absorption mechanisms in 20 kW-classCO2 laser welding processes.J.Phys.D:Appl.Phys.36(2003)pp.192-203

[22] ChengY.,X. Jin, S. Li,L. Zeng, Fresnel absorption and inverse bremsstrahlung absorption in anactual 3D keyhole during deep penetration CO2 laser welding of aluminum 6016,Optics & Laser Technology, 44 (2012) pp. 1426–1436

[23] Finke BR, Kapadiat PD, Dowden JM. A fundamental plasma based model for energy transfer in laser material processing. Journal of Physics D: Applied Physics 1990;23:643–54.

[24] Lacroix D, Jeandel G. Spectroscopic characterization of laser-induced plasma created during welding with a pulsed Nd:YAG laser. Journal of Applied Physics 1997;81:6599–606.

[25] Zhang Y, Li L, Zhang G. Spectroscopic measurements of plasma inside the keyhole in deep penetration laser welding. Journal of Physics D: Applied Physics 2005;38:5.

[26] Zhang Y, Chen G, Li L. Design for Measurements of Electron and Density of Laser Induced Plasma. Manufacturing Technology and Machine Tool 2008;3:98–101

[27] SibillanoT,et al. Study on the correlation between plasma electron temperature and penetration depth in laser welding processes. Physics Procedia 2010;5:429–36.

[28] D'AngeloCA,Pace DMD, Bertuccelli G.Semiempirical model for analysis of inhomogeneous optically thick laser-induced plasmas. Spectrochimica Acta Part B2009;64:999–1008.

[29] QiJ.,et al. The influence of process parameters on plasma temperature during CO2 laser welding aluminum alloy. Transactions of the China welding institution 2008;29(6):97–100.

[30] Beck M,Berger P,Hugel H.The effect of plasma formation on beam focusing in deep penetration welding with CO2 lasers. Journal of PhysicsD: Applied Physics 1995;28:2430–42.

[31] ElhassanA, et al. Effect of applying static electric field on the physical parameters and dynamics of laser-induced plasma. Journal of Advanced Research 2010;1:129–36.

[32] Sibillano T, et al. A study of the shielding gas influence on the laser beam welding of AA5083 aluminium alloys by in-process spectroscopic investigation. Journal of Physics D: Applied Physics 2006;44:1039–51.

[33] Bhatti KA, et al. Electrons emission from laser induced metallic plasmas. Vacuum 2010;84:980–5.

[34] Djebli M, Marif H. Adiabatic dust-acoustic double layers in two temperature electron dusty plasma. Physics Letters A 2009;373:2572–6.

[35] Dilthey U, et al. Kinetic description of keyhole plasma in laser welding. Journal of PhysicsD:Applied Physics2000;33:2747–53.

[36] M. Gao, C.Chen, M.Hu, L. Guo, Z. Wang, X. Z. Wuhan, Characteristics of plasma plume in fiber laser welding of aluminum alloy, Applied Surface Science 326 (2015) 181–186

[37] Y. Zhang , S. Li,G.Chen,H. Zhang,M. Zhang, Characteristics of zinc behavior during laser welding of zinc ''sandwich'' sample, Optics & Laser Technology 44 (2012) pp.2340–2346

[38] F. Kong , J.Ma, B.Carlson , R. Kovacevic, Real-time monitoring of laser welding of galvanized high strength steel in lap joint configuration, Optics & Laser Technology 44 (2012) 2186–2196

[39] Yue Wu , Y. Cai, D. Sun , J. Zhu, Yi. Wu, Characteristics of plasma plume and effect mechanism of lateral restraint during high power CO2 laser welding process, Optics & Laser Technology64(2014) pp.72–81

[40] ZhangW., X. Hua , W. Liao , F. Li , M. Wang, The effect of the welding direction on the plasma and metal transfer behaviorofCO2 laser + GMAW-Phybrid welding processes, Optics and Lasers in Engineering 58(2014) pp. 102–108

[41] Sibillano T., D. Rizzi , A. Ancona, S. Saludes-Rodil, J. Rodriguez Nieto,H. Chmelickova, H. Sebestova, Spectroscopic monitoring of penetration depth in CO2 Nd:YAG and fiber laser welding processes, Journal of Materials Processing Technology 212 (2012) 910–916

[42] Wang J.,Ch.Wangn, X. Meng,X. Hu,Y.Yu,Sh.Yu, Study on the periodic oscillation of plasma/vapour induced during high power fibre laser penetration welding, Optics & Laser Technology 44 (2012) 67–70

[43] Schmidt M,Otto A,Kägeler C.Analysis of Yag laser lap-welding of zinc coated steel sheets. CIRP Ann. Manuf. Technol. 2008;57/1:pp213–6.

[44] Kumar N., S.Dash, A.K.Tyagi and B.Raj, Keyhole depth instability in case of CW CO2 laser beam welding of mild steel, Sadhana, v.35, p.10,2010, pp.609-618, Indian Academy of Sciences

[45] Sibillano T., A.Ancona, D.Rizzi, V.Lupo, L.Tricarico and P.M.Lugara A plume oscillations monitoring during Laser welding of Stainless steel by discrete Wavelet transform application, Sensors, 10, 2010, pp.3549-3561

[46] Wang J., Ch. Wang, X. Meng, X. Hu,Y. Yu,Sh. Yu, Study on the periodic oscillation of plasma/vapor induced during high power fibre laser penetration welding, Optics &LaserTechnology44(2012)pp. 67–70

[47] Kaplan A., P.Norman, I.Eriksson, Analysis of the Keyhole and Weld Pool Dynamics by Imaging Evaluation and Photodiode Monitoring, Proceedings of LAMP2009-the 5th International Congress on Laser Advanced Material Processing, pp.1-6

[48] Li. G., Y. Cai, Y. Wu, Stability information in plasma image of high-power CO2 laser welding, Optics and Lasers in Engineering 47 (2009) pp. 990–994

[49] Tenner F., C.Brock, F.Klämpfl, M.Schmidt, Analysis of the correlation between plasma plume and keyhole behavior in laser metal welding for the modeling of the keyhole geometry, Optics and Lasers in Engineering64(2015) pp.32–41

[50] YouD. Y., X. D. Gao and S. Katayama, Review of laser welding monitoring, Science and technology of welding & joining · 2014, DOI: 10.1179/1362171813Y.0000000180

[51] You D., X. Gao and S. Katayama: Multiple-optics sensing of high-brightness disk laser welding process, NDT & E Int., 2013,60, 32–39.

[52] Eriksson I., J. Powell and A. F. H. Kaplan: Signal overlap in the monitoring of laser welding, Meas. Sci. Technol., 2010, 21,105705.

[53] Na X., Y. Zhang, Y. S. Liu and B. Walcott, Nonlinear identification of laser welding process, IEEE Trans. Control Syst. Technol., 2010, 18, 927–934.

[54] PengY.,W.Chen, Ch.Wang, G. Bao and Zh. Tian, Controlling the plasma of deep penetration laser welding to increase power efficiency, J. Phys. D: Appl. Phys. 34 (2001) 3145–3149

[55] Liy L., D. J. Brook fieldz and W. M. Steen, Plasma charge sensor for in-process, non-contact monitoring of the laser welding process, Meas. Sci. Technol., 1996, 7, 615–626.

[56] Y. M. Zhang, S. B. Zhang and Y. C. Liu, A plasma cloud charge sensor for pulse keyhole process control, Meas. Sci. Technol., 2001, 12, 1365–1370.

[57] Baschenko, VW, Mauer, K.-O. Untersuchungen zur Durchdringungs und Rückstreus- trahlung aus dem Dampfkanal beim Elektronenstrahlschweisen //ZIS-Mitteilungen. – 1976. – Nr. 9. – S. 923-936.

[58] Mauer, K.O., 1976. A method and device for charged particles flow control, Patent No119363/20.04.1976, Germany.

[59] Kirczuk, Cz., 1979. Metodakontroliogniskowaniawiazkielektronowej w procesie spawania elektronowiazkowego. ITE P. Wr., Wroclaw (in Polish).

[60] Olszewska, K., Friedel, K., 2004. Control of the electron beam active zone position in electron beam welding processes. Vacuum 74, 29–43.

[61] Leskov, G.I., Nesterenkov, V.M.,1988. Control of electron beam through plasma parameters,. In: Proceedings of the Second international conference on electron beam technologies, Varna May 31–June 4. Publisher IE BAS, Sofia, pp. 106–112 (in Russian).

[62] Nesterenkov, V.M., 1982. Effect of the ion current on weld geometry parameters at electron beam melting. Automat. welding, 34–36 (In Russian)

[63] D.TrushnikovD., G.Mladenov, V.Belenkiy, E.Koleva, Ion current collected from generated plasma during EBW, Elektrotechnica &Elektronica, v.56, No 5-6, pp 22-29, 2014, Sofia, Publ. CEEC, ISSN 0861-4717

[64] TrushnikovD. N. and G. M. Mladenov, Numerical model of the plasma formation at electron beam welding, Journalof Applied Physics 117, 1, (2015), DOI: 10.1063/1.4905193

[65] Belen'kii V. Ya., V. M. Yazovskikh, A.P. Zhuravlev, Nature of the secondary current in the plasma formed in the zone affected by the electron beam during welding, Physics and Chemistry of Materials Treatment. 6, (1983), pp.128-131 (In Russian).

[66] Yazovskikh V.M., Belenkiy V.Ya. Control of electron beam welding using plasma phenomena in the molten pool region // Weld. Int. – 1997. – Vol. 11. – pp. 554–558.

[67] Trushnikov D. N., V. Ya. Belen'kiy, V.M.Yazovskikh, L.N.Krotov, Formation of a secondary-emission signal in electron beam welding with continuous penetration, Welding International, 21, 5, (2007),pp.384-386.

[68] TrushnikovD.N., V.Ya. Belen'kiy , V.M.Yazovskikh, L.N.Krotov, Formation of a secondary-emission signal in electron beam welding with continuous penetration, Welding International, 21, 5, 2007,pp.384-386

[69] TrushnikovD.N., G.M. Mladenov, V.Y. Belenkiy, E.G. Kolevaand S. V. Varushkin, Current-driven ion-acoustic and potential-relaxation instabilities excited in plasmaplume during electron beam welding, AIP Advances, 2014,V. 4, 4, doi: 10.1063/1.4870944

[70] UglovA.A., S.B.Selisthev, Avtho-oscillating processes at interaction of concentrated energy flows, Moskow,Science, (1987), In Russian.

[71] BashenkoV. V., D. I. Ivanov, E. A. Mitkevich, G. A. Turichin, Physical model of electron energy transport at electron beam welding, Second International Conference on Electron Beam Technologies, Varna, 31,05-4,06, 1988, Publisher Institute of electronics BAS, Sofia, (1988), pp. 464-471 , In Russian.

[72] Li L., D.Brookfield, W.Steen, Plasma charge sensor for in-process, non-contactmonitoring of the welding process. Meas.Sci.,Technol.,7,(1996), pp.615-626.

[73] TrushnikovD., V.Belenkiy, V. Shchavlev, A. Piskunov, A. Abdullin and G.Mladenov, Plasma Charge Current for Controlling and Monitoring Electron Beam Welding with Beam Oscillation, Sensors,2012, 12, 17433-17445; doi:10.3390/s121217433

[74] TrushnikovDN, VE Shchavlev, GM Mladenov, LN Krotov: Chapter: Investigation of Processes in the Keyhole of Electron-Beam Welding by Monitoring the Secondary Current Signal in the Plasma, pp.217-230 in book: "In-situ Studies with Photons, Neutrons and Electrons Scattering II", Kannengiesser, Th., Babu, S.S., Komizo, Y.-i., Ramirez, A. (Eds.) 259 p.DOI: 10.1007/978-3-319-06145-013,Springer International Publishing,Switzerland 2014

[75] KolevaE.G., G.M.Mladenov, D.N.Trushnikov, V.Ya.Belenkiy, Signal emitted from plasma during electron-beam welding with deflection oscillations of the beam. J.of Materials Processing Technology, 214, 2014, pp. 1812-1819

[76] Trushnikov D.N., Dissertation, 2016, National Research Polytechnic University of Perm, Perm. Russian Federation

[77] Rai, R., Palmer, T. A., Elmer, J. W., & Debroy, T. (2009). Heat transfer and fluid flow during electron beam welding of 304L stainless steel alloy // Weld. J. – 2009. – Т.88. – №3. – 54s-61s.

[78] Trushnikov D. N., Salomatova E. S., Belenkiy V. Y. Estimation of the Temperature in the Weld Penetration Channel in Electron Beam Welding //Journal of Power and Energy Engineering. – 2013. – Т. 1. – №. 07. – С. 51.